Report to the 1964
Dubna Conference

CERN/TC/PHYSICS 64-18
1.6.1964

Not for Publication

$Y\bar{Y}$ PRODUCTION BY 5.7 GEV/C ANTIPROTONS IN HYDROGEN

R. Bock, A. Cooper, B.R. French, R. Levi Setti*,

CERN, Geneva

and

D. Revel, B. Tallini, S. Zylberajch,

C.E.N., Saclay.

INTRODUCTION

The 81cm Saclay hydrogen bubble chamber was exposed to $4 \cdot x10^6$ antiprotons of 5.7 GeV/c. The spread in the beam momentum was estimated at $\pm 1^o/o$. The contamination of the beam, obtained from δ-ray counting, was $6^o/o$ μ's and $2^o/o$ π's. A value of 0.0625 gm/cm^3 has been used for the density of liquid hydrogen in the computation of cross-sections.

Presented here are the preliminary results, derived from half the available data, concerning hyperon-antihyperon production in two, three, four and five-body final states. Results on similar works at 3, 3.6 and 4 GeV/c antiproton momenta have been reported elsewhere(1).

The cross-sections for the various reaction channels studied here are summarised in Table 1.

I. $Y\bar{Y}$ FINAL STATES

The Δ^2 distribution for the two-body reactions $\Lambda\bar{\Lambda}$, $\Lambda\bar{\Sigma^o}$, and $\Sigma^+\bar{\Sigma^+}$ are shown in Fig.1. A common feature is the peaking of the distributions at low Δ^2 values, corresponding to the strong forward (backward) collimation of the antihyperons (hyperons) in the c.m.s.

While for $\Lambda\bar{\Lambda}$ the fraction of events having $\Delta^2 > 0.25$ is ~0.25 for the $\Lambda\bar{\Sigma^o}$ and the $\Sigma^+\bar{\Sigma^+}$ this fraction becomes 0.5 and 0.6, respectively.

---

* Guggenheim Fellow, on leave of absence from the University of Chicago

Thus the general character of the production mechanism is similar to that observed in the region of 3 to 4 GeV/c. However, we note that in the present set of data there is no evidence for $\Sigma^-\bar{\Sigma}^-$ production.

The high $\Sigma^+\bar{\Sigma}^+$ cross-section relative to that for $\Sigma^-\bar{\Sigma}^-$ production on one side, and the strong forward (backward) collimation of the antibaryons (baryons) on the other, are suggestive of an exchange production mechanism, where the contribution of the exchange of a charge Q = 2, strangeness S = 1 system is small compared with that of Q = 0,1 systems.

II. $Y\bar{Y}\pi$ AND $\bar{Y}KN$ FINAL STATES

(1) $\Lambda^o\bar{\Lambda}^o\pi$ events :- The Dalitz plot of Figure 2 shows that these events proceed mainly via the quasi-two-body reaction $p\bar{p} \rightarrow \Lambda\bar{Y}^{*}$ + c.c. with $\sim 65^o/o$ $Y_1^*(1385)$ and $\sim 22^o/o$ $Y^*(1660)$. The Δ^2 distribution, for the $Y_1^*(1385)$ producing reactions, of Figure 1d. is similar to those for the two-body $Y\bar{Y}$ events.

(2) $\Sigma^+\bar{\Lambda}\pi^-$ + c.c. and $\Sigma^-\bar{\Lambda}\pi^+$ + c.c. Evidence for the production of $Y_1^*(1385)$ and some $Y_o^*(1405)$/and $Y_o^*(1520)$ resonances in these reactions is exhibited in the Dalitz plot shown in Figure 3.

Several of the features of these reactions can be understood in terms of the exchange mechanism mentioned above, viz.,

a) once again the antihyperons show a strong forward peaking in the C.M.S.

b) in the reaction $\Sigma^-\pi^+\bar{\Lambda}$ + c.c. the $\bar{Y}_1^{*-} \rightarrow \bar{\Lambda}+\pi^+$, corresponding to the Q = 2 exchange in the above model, is absent

c) after subtraction of the $Y_1^*(1385)$, $Y_o^*(1405)$/and $Y_o^*(1520)$ contributions the ratio $\sigma(\Sigma^+\pi^-\bar{\Lambda})/\sigma(\Sigma^-\pi^+\bar{\Lambda})$ equals about 3

d) in those reactions where a Σ^o replaces the Λ^o we find $\sigma(\Sigma^+\pi^-\bar{\Sigma}^o)/\sigma(\Sigma^-\pi^+\bar{\Sigma}^o)$ about 2.5

e) for the four-body reactions, where an extra π^o is produced, the ratio $\sigma(\Sigma^+\pi^-\bar{\Lambda}^o\pi^o)/\sigma(\Sigma^-\pi^+\bar{\Lambda}^o\pi^o)$ also equals about 2.5.

(3) $\Lambda K^{+}\bar{p}$ + c.c. and $\Lambda K^{o}\bar{n}$ + c.c. The only significant departure from a uniform population of the Dalitz plots in these reactions is observed in the region of the $Y_o^*(1520)$ as can be seen in Figure 4.

III. $Y\bar{Y}\pi\pi$ FINAL STATES

$\Lambda\bar{\Lambda}\pi^{+}\pi^{-}$: This channel is dominated by the production of Y_1^*, $(\bar{Y}_1^*)$ via a peripheral-type mechanism. Thus the M ($\Lambda\pi$, $\bar{\Lambda}\pi$) vs. cos $\theta^*_{\Lambda\pi}$ plot of Figures 5a and 5b shows a strong enhancement in the Y_1^* region at large cos $\theta^*_{\Lambda\pi}$ values, together with an essentially complete forward-backward asymmetry in the repartition of the $\bar{\Lambda}\pi$ and $\Lambda\pi$ momentum vectors, respectively. Moreover, the excess of $Y_1^{*+}(\overline{Y_1^{*+}})$ over the $Y_1^{*-}(\overline{Y_1^{*-}})$, ap arent in the mass plots of Figures 5b and 5c, can be entirely accounted for by an excess of associated production of $Y_1^{*+}\,\overline{Y_1^{*+}}$ pairs. Evidence for associated $Y_1^*\bar{Y}_1^*$ production is contained in Figures 6a and 6b, where the population of points in the crossing Y_1^*, $\bar{Y}_1^*$ bands is enhanced with respect to that expected from the background contribution.
In more detail, there are 25 events of the type $Y_1^{*+}\overline{Y_1^{*+}}$ versus 12 $Y_1^{*-}\overline{Y_1^{*-}}$ while the background is unlikely to exceed 6 of each type. This yields a ratio $Y_1^{*+}\overline{Y_1^{*+}}\,/Y_1^{*-}\,\overline{Y_1^{*-}}$ of 19/6.

We acknowledge the assistance of the CERN proton synchrotron staff, members of the CERN Track Chambers Division who built the separated beam and the crew of the 81cm Saclay bubble chamber.

The Saclay group wishes to thank Drs. G.P. Porte and A. Verglas for their help in the programming.

TABLE 1

	Reaction	σ(μbs)
1.	$p\bar{p} \rightarrow \Lambda^{o}\bar{\Lambda}^{o}$	40 ± 10
2.	$\Lambda^{o}\bar{\Sigma}^{o}$ + c.c.	30 ± 8
3.	$\Sigma^{+}\bar{\Sigma}^{+}$	37 ± 10
4.	$\Sigma^{-}\bar{\Sigma}^{-}$	2 ± 6
5.	$\Sigma^{+}\Lambda^{o}\pi^{-}$ + c.c.	45 ± 8 → ~12 $\Sigma^{+}\bar{Y}_{1}^{*+}(1385)$+cc; → ~6 $\Lambda\,\bar{Y}_{o}^{*}(1405)$+cc
6.	$\Sigma^{-}\bar{\Lambda}^{o}\pi^{+}$ + c.c.	20 ± 5 → ~1 $\Sigma^{-}\bar{Y}^{*-}(1385)$+cc; → ~5 $\Lambda\,Y_{o}^{*}(1405)$+cc
7.	$\Sigma^{+}\bar{\Sigma}^{o}\pi^{-}$ + c.c.	25 ± 7
8.	$\Sigma^{-}\bar{\Sigma}^{o}\pi^{+}$ + c.c.	10 ± 4
9.	$\Lambda^{o}\bar{\Lambda}^{o}\pi^{o}$	78 ± 13 → ~50 $\Lambda\bar{Y}_{1}^{*}(1385)$+cc; → ~16 $\Lambda\bar{Y}^{*}(1660)$+cc
10.	$\Lambda^{o}K^{o}\bar{n}$ + c.c.	$60 \pm 16 \rightarrow$ ~7 $\Lambda\bar{Y}_{o}^{*}(1520)$+cc
11.	$\Lambda^{o}K^{+}\bar{p}$ + c.c.	$29 \pm 6 \rightarrow$ ~6 $\Lambda\bar{Y}_{o}^{*}(1520)$+cc
12.	$\Sigma^{o}K^{+}\bar{p}$ + c.c.	13 ± 5
13.	$\Sigma^{+}K^{o}\bar{p}$ + c.c.	20 ± 8
14.	$\Sigma^{+}\bar{\Lambda}^{o}\pi^{-}\pi^{o}$ + c.c.	41 ± 8
15.	$\Sigma^{-}\bar{\Lambda}^{o}\pi^{+}\pi^{o}$ + c.c.	19 ± 5
16.	$\Sigma^{o}\bar{\Lambda}^{o}\pi^{+}\pi^{-}$ + c.c.	16 ± 4
17.	$\Lambda^{o}\bar{\Lambda}^{o}\pi^{+}\pi^{-}$	27 ± 5
18.	$\Sigma^{+}\pi^{-}\bar{K}^{o}n$ + c.c.	40 ± 10
19.	$\Sigma^{+}\bar{p}\,K^{o}\pi^{o}$ + c.c.	24 ± 8
20.	$\Lambda^{o}\bar{\Lambda}^{o}\pi^{+}\pi^{-}\pi^{o}$	43 ± 9

PS/4394/mhg

Figure Captions

Figure 1 — $-\Delta^2$ distributions for $\bar{p}p$ reactions leading to two-body final states.

Figure 2 — Dalitz plot for $\bar{p}p \rightarrow \Lambda\bar{\Lambda}\pi^0$ events. The phase space mass distribution, outside of the $Y_1^*(1385)$ bands, is indicated by the dashed line in b).

Figure 3 — Dalitz plot for $\Sigma\bar{\Lambda}\pi$, $\bar{\Sigma}\Lambda\pi$ final states.

Figure 4 — Dalitz plot for $A\bar{N}K$, $\bar{A}N\bar{K}$ final states.

Figure 5 — Scatter plot of the invariant $\Lambda\pi$, $(\bar{\Lambda}\pi)$ mass versus $\cos\theta^*_{\Lambda\pi}$ for $\Lambda\bar{\Lambda}\pi^+\pi^-$ events.

Figure 6 — Correlation plot between the $\Lambda\pi^+(\bar{\Lambda}\pi^-)$ and $\bar{\Lambda}\pi^+(\Lambda\pi^-)$ invariant-mass combinations for $\Lambda\bar{\Lambda}\pi^+\pi^-$ events.

RS/4394/mhg

FIG. 1

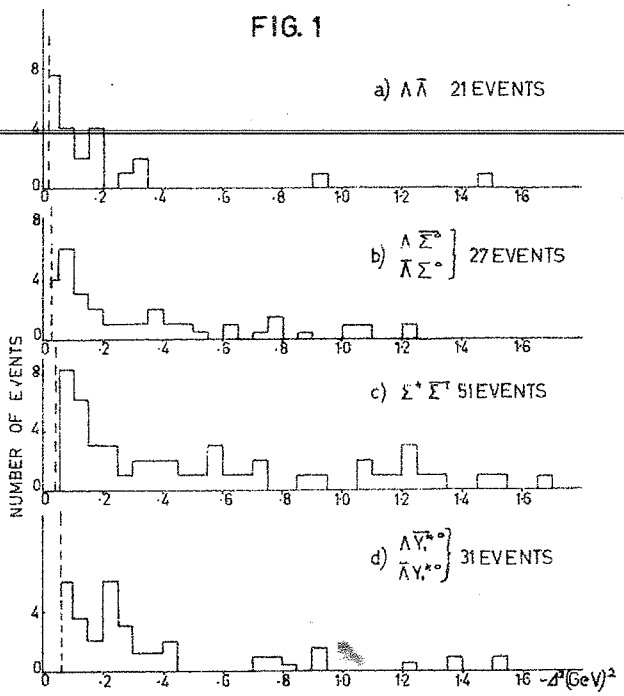

DIA 20677

FIG. 2

a)
Λ Λ̄ π⁰
45 EVENTS

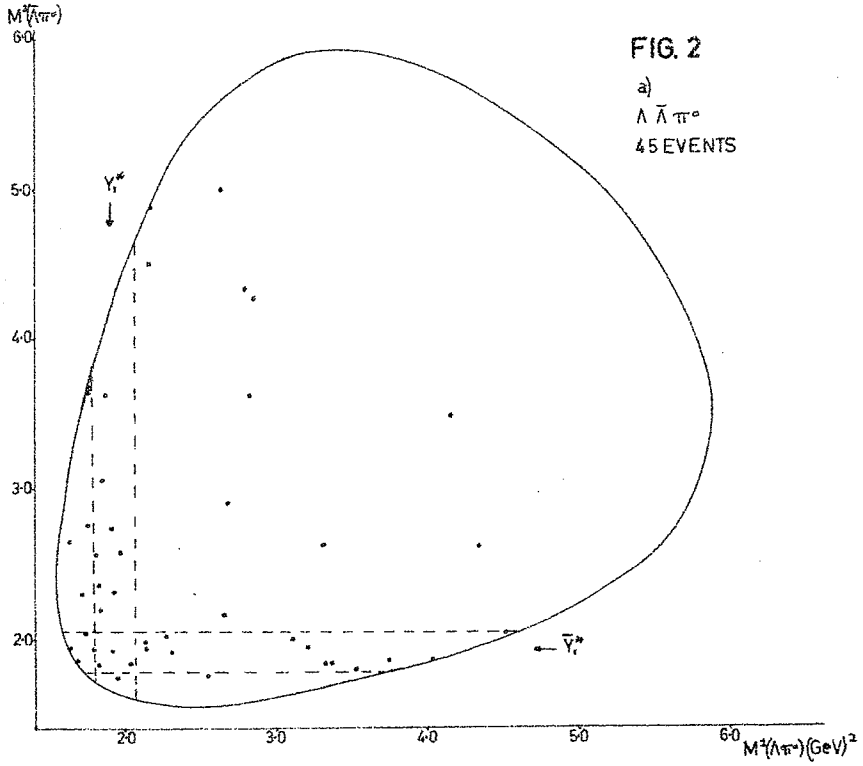

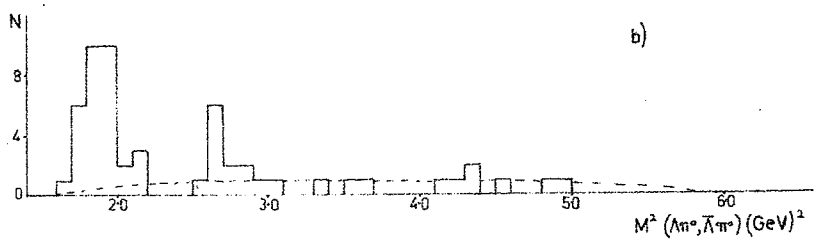

DIA 20678

PS/4394

FIG. 3

DIA · 2/158

FS/439#

FIG. 4

DIA 21157

PS/4394

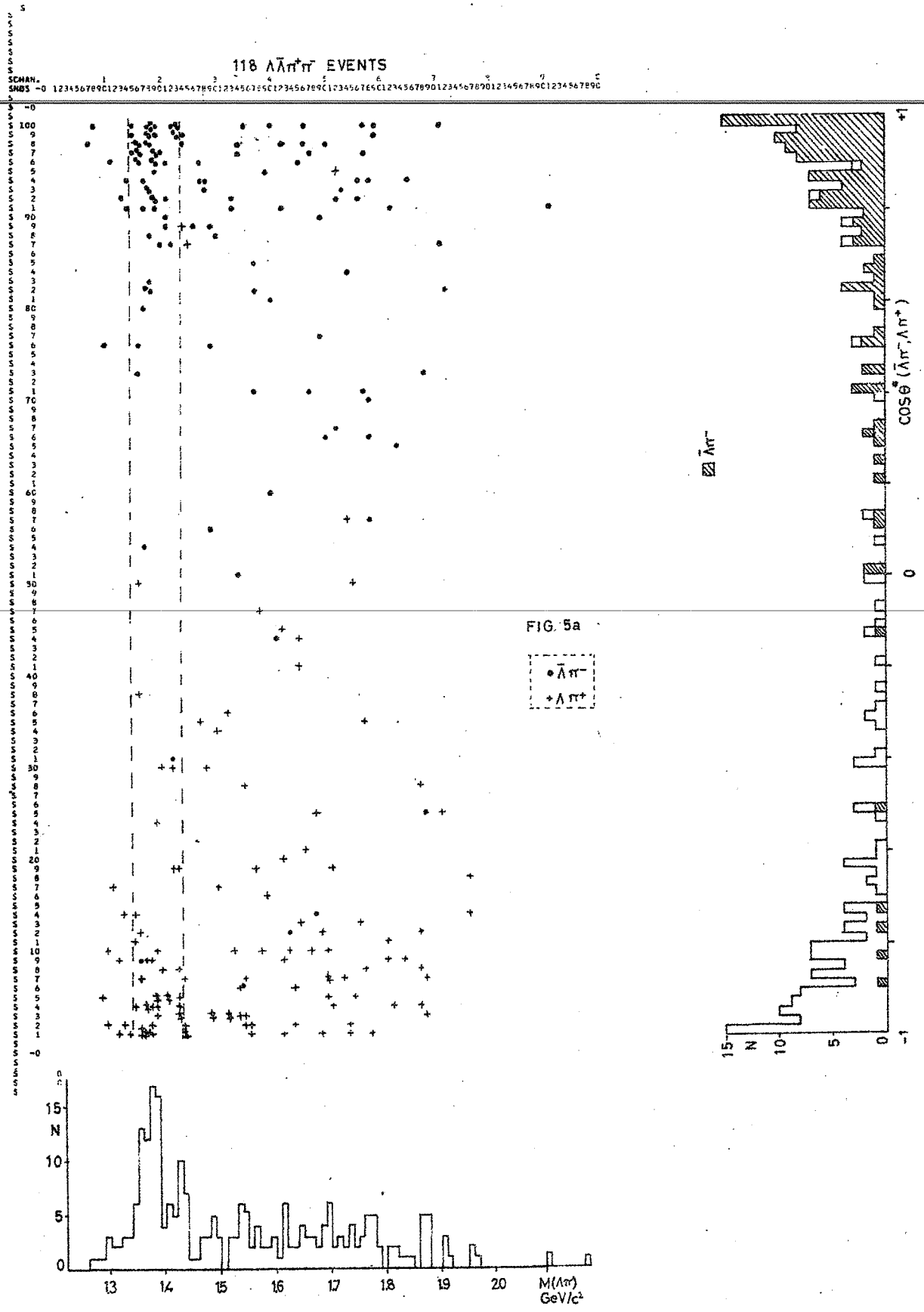

FIG. 5a

DIA 21155

PS/4394

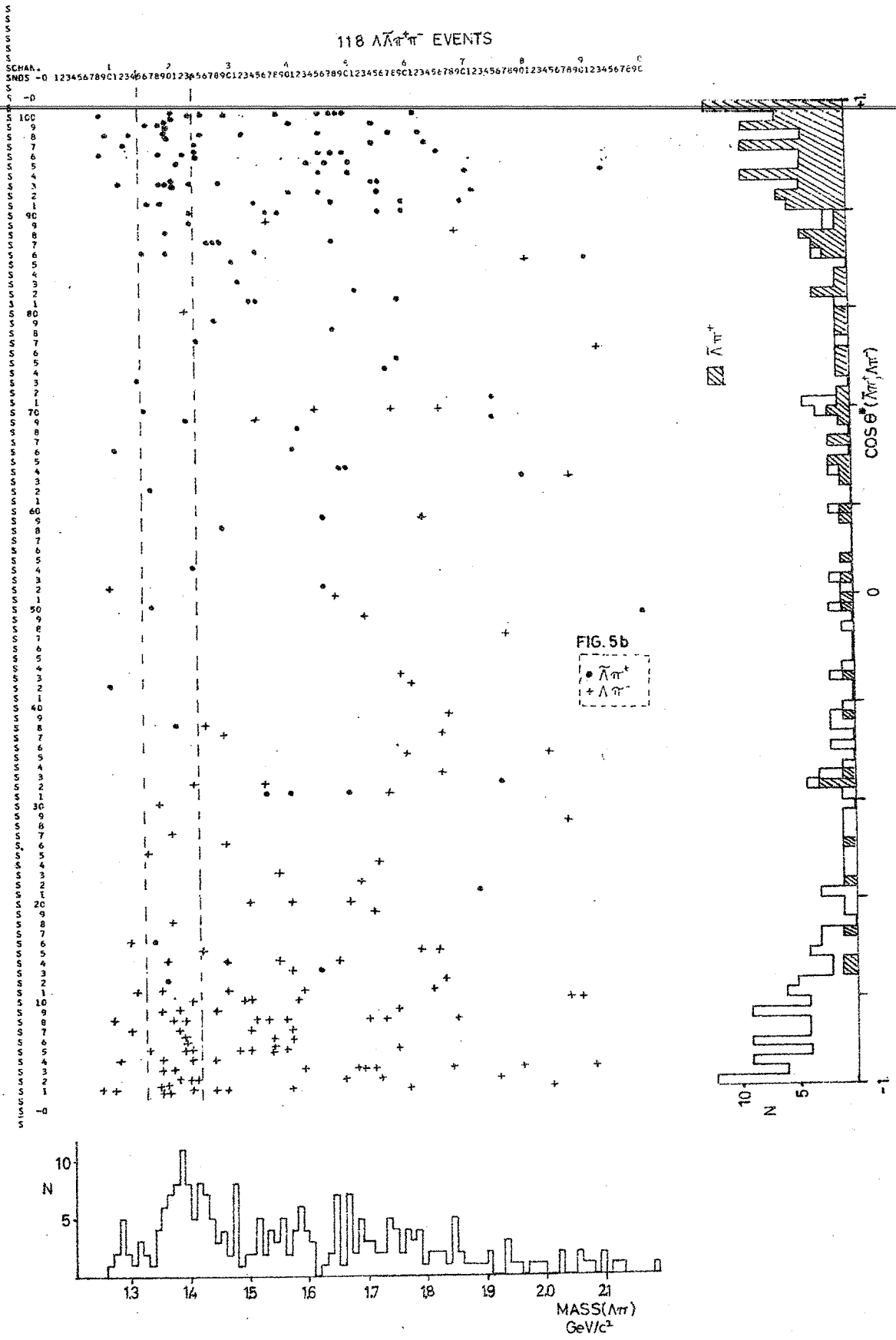

DIA 21156

PS/4394

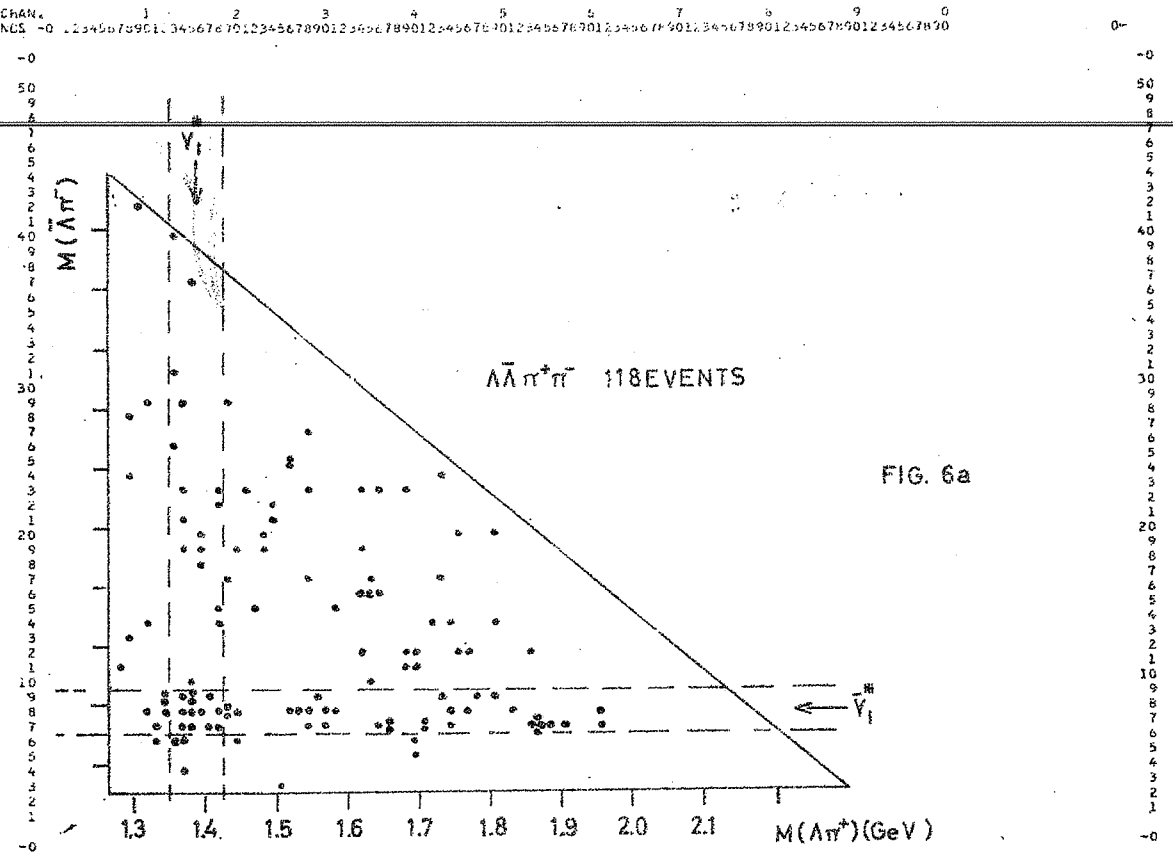

FIG. 6a

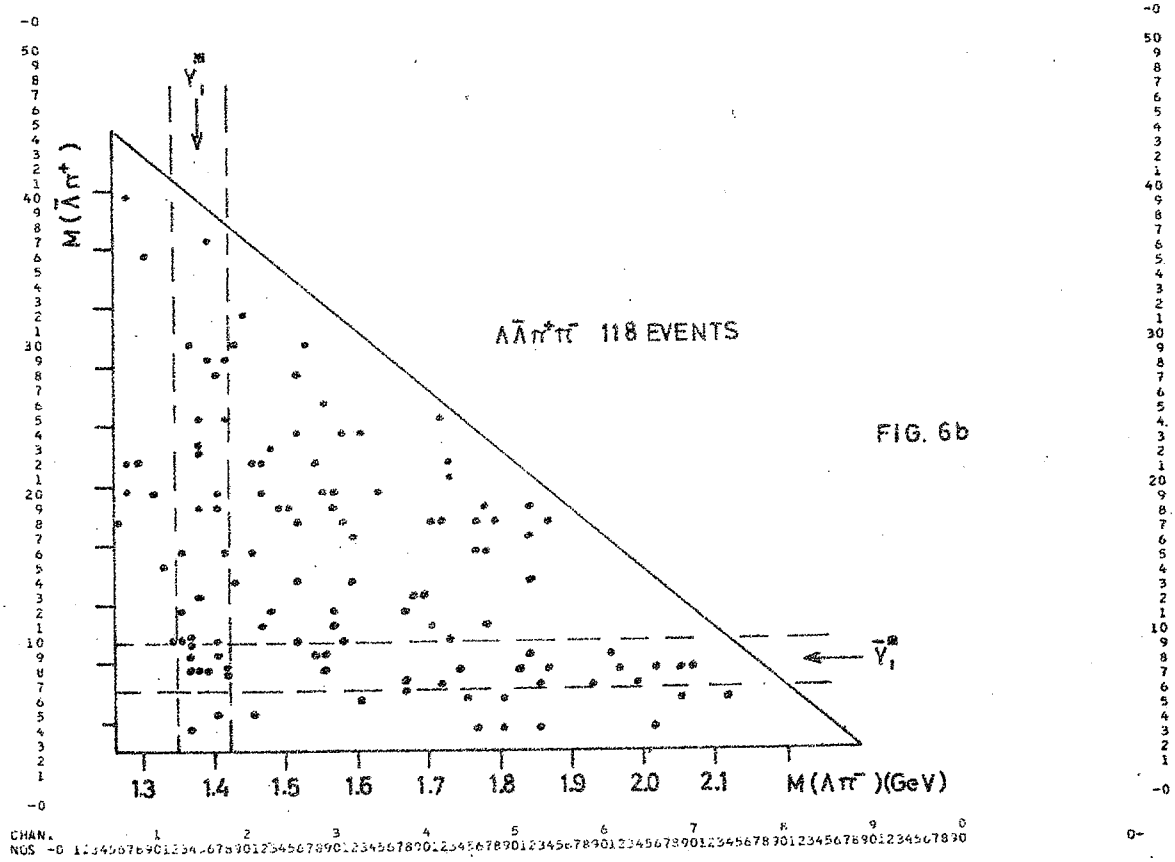

FIG. 6b

DIA 2/159

PS/4394